

Physicochemical properties and feasibility of coconut oil-based diacylglycerol as an alternative fat for healthy non-dairy creamer

Xuan Liu^{a,1}, Wanli Xu^{a,1}, Weifei Wang^b, Riming Luo^c, Bo Yang^d, Dongming Lan^{a,*}, Yonghua Wang^{a,e,*}

^a School of Food Science and Engineering, South China University of Technology, Guangzhou 510640, China

^b Sericultural & Argi-Food Research Institute, Guangdong Academy of Agricultural Sciences/Key Laboratory of Functional Foods, Ministry of Agriculture and Rural Affairs/Guangdong Key Laboratory of Agricultural Products Processing, No. 133 Yiheng Street, Dongguan Zhuang Road, Tianhe District, Guangzhou 510610, China

^c Guangdong Yue-shan Special Nutrition Technology Co., Ltd., Foshan 528000, China

^d School of Bioscience and Bioengineering, South China University of Technology, Guangzhou 510006, China

^e Guangdong Youmei Institute of Intelligent Bio-manufacturing Co., Ltd, Foshan 528200, China

ARTICLE INFO

Keywords:

Coconut oil-based diacylglycerol
Non-dairy creamer
Physicochemical characteristic
Trans fatty acids
Black coffee

ABSTRACT

Non-dairy creamers have been widely used for coffee whitening and texture improvement. To avoid the intake of trans fatty acids from partially hydrogenated oil, coconut oil-based diacylglycerol (CO-DAG) was applied in non-dairy creamer as core material. In this study, effects of DAG content (30, 50, 70, 90%) on the characteristics of CO-DAG were evaluated, including rheological and thermodynamic properties. The CO-DAG with a content of 50% exhibited a wide plastic range and contained mixture of β and β' polymorphic forms. Using CO-DAG (50%) as core material, the physicochemical properties of non-dairy creamer were characterized and compared with commercial products. The results indicated that CO-DAG-based non-dairy creamers showed similar encapsulation efficiency (92.74%) and thermal stability to commercial products. Furthermore, CO-DAG-based non-dairy creamer showed higher whiteness index (54.20) than commercial non-dairy creamers (50.22) when applied to black coffee. Overall, it is anticipated that CO-DAG-based non-dairy creamers have great potentials in coffee whitening.

Introduction

Non-dairy creamers, also called coffee creamers, or coffee whiteners, are microencapsulated powders containing syrups, edible oils (partially hydrogenated soybean or rapeseed oil), sodium caseinate and other ingredients, which are widely used for whitening and texture improvement of coffee (Wanthong, & Klinkesorn, 2020). The non-dairy creamer market is facing significant challenges with consumers' increasing pursuit of healthy and functional products. Unfortunately, current commercial non-dairy creamers using partially hydrogenated vegetable oils as core material pose great health threats specifically due to the issues of trans fatty acids (Dhaka, Gulia, Ahlawat, & Khatkar, 2011). It has been sufficiently documented that excessive intake of trans fatty acids would significantly increase the risk of cardiovascular disease, type 2 diabetes and cancer (Islam, Amin, Siddiqui, Hossain, Sultana, & Kabir, 2019). Therefore, there is an urgent demand for healthy non-dairy creamer

alternatives.

Coconut oil (CO) is rich in medium-chain fatty acid (MCFA, C6-C12), including lauric acid, caprylic acid and capric acid, which has physiological benefits in anti-inflammatory, prevention of cardiovascular disease and Alzheimer's disease (Teng, Zhao, Khoo, Yeo, Yong, & Lim, 2020; Ramesh, Krishnan, Praveen, & Hebbar, 2021). Diacylglycerol (DAG) oils represent a kind of healthy oils with potential functions in control of postprandial lipid levels and prevention of body fat accumulation compared with triacylglycerols (TAGs) (Lee, Zhang, Lai, Tan, & Wang, 2020). It is demonstrated that the enzymatically produced coconut oil-based diacylglycerol (CO-DAG) could significantly reduce serum triglyceride content, body weight and the level of hepatic fatty acid synthase compared with CO (Lu, Guo, Fan, Deng, Luo, & Li, 2020).

Admittedly, the melting point and solid fat content (SFC) of core material play a key role in the stability of non-dairy creamer. In general, vegetable oils (soybean oil, palm oil, coconut oil) as core material have

* Corresponding authors at: School of Food Science and Engineering, South China University of Technology, Guangzhou 510640, China (Y. Wang).

E-mail addresses: dmlan@scut.edu.cn (D. Lan), yonghw@scut.edu.cn (Y. Wang).

¹ Equal contribution.

relatively low melting point and need to be partially hydrogenated to increase their melting point. Nowadays, hydrogenated soybean oil and soybean oil catalyzed by enzymatic interesterification (Wang & Liu, 2014), palm olein (Soo, Tan, Tan, Khalid, & Tan, 2021) and rambutan kernel olein (Wanthong, & Klinkesorn, 2020) are used as core material instead of hydrogenated vegetable oil to improve the stability of non-dairy creamer. Our previous study showed that DAGs have higher SFC and melting point compared with TAGs (Liu et al., 2022). Till now, the application of CO-DAG in non-dairy creamer can be hardly found. It is speculated that the non-dairy creamers using CO-DAG as core material have great potentials not only in prevention of body fat accumulation but also in avoidance of health problems caused by excessive intake of trans fatty acids.

Hence, the aim of this study is to develop CO-DAG-based non-dairy creamers, and to evaluate the physicochemical properties and applications. The effects of CO-DAG concentrate (30, 50, 70, 90%) on the physicochemical properties were investigated, including melting point, SFC, thermodynamic properties and crystal polymorphism. Then the non-dairy creamer was prepared with CO-DAG at a content of 50% as core material. The properties of CO-DAG-based non-dairy creamer were characterized and compared with commercial products. Finally, its application in black coffee was evaluated.

Materials and methods

Materials

CO and commercial non-dairy creamer were obtained from local supermarket (Guangzhou, Guangdong, China). CO-DAG was provided by Guangdong Yue-shan Special Nutrition Technology Co., Ltd (Foshan, Guangdong, China). The oligosaccharides were purchased from Guangdong Huasheng Food Co., Ltd. (Guangzhou, Guangdong, China). Sodium caseinate and monostearate glycerides were obtained from Guangdong Xingda Food Ingredients Co., Ltd. (Guangzhou, Guangdong, China). Glycerol trioleate (>99%), 1,3-Dioleoylglycerol (>95%), 1,2-Dioleoylglycerol (>98%) and 1-oleoyl-*rac*-glycerol (>99%) were provided from Anpel Laboratory Technologies Inc (Shanghai, China). HPLC grade methanol, 2-propanol, *n*-hexane, acetonitrile and formic acid were obtained from Kermel Chemical Reagent Factory (Tianjin, China). Thirty-seven fatty acid methyl esters (FAMES), monoolein (>99%) and all other chemicals were obtained from Sigma-Aldrich (St. Louis, MO, USA).

Fatty acid composition analysis

The fatty acid composition and trans fatty acids were measured using an Agilent 7890A GC system (Agilent Technologies, Palo Alto, CA, USA) equipped with a capillary CP-Sil 88 column (60 m × 0.25 mm, 0.2 μm film thickness). The sample was methylated to FAMES according to a previously described method (Xu et al., 2022). The 60 mg oil was dissolved in isoctane (4 mL), then a potassium hydroxide-methanol solution (200 μL) was added for methyl esterification. Finally, the sample was analyzed by GC. The split ratio was 30:1. The detector and initial temperature were 280 and 250 °C, respectively. The column temperature was increased from 140 °C to 200 °C at a rate of 4 °C/min for 2 min, and then increased to 220 °C at a rate of 2 °C/min for 18 min, and finally increased 230 °C at a rate of 10 °C/min for 10 min. FAMES were identified by comparing their retention times with standards and quantified through the peak area normalization method. The detailed analytical conditions refer to the method (Wang, Qin, Li, Yang, & Wang, 2017).

Acylglycerols analysis

The acylglycerol composition was determined by high performance liquid chromatography (HPLC) equipped with a refractive index detector (RID, Waters 2414, Milford, USA) on a Phenomenex Luna silica

column (250 mm × 4.6 mm, 5 μm particle size) according to a previous method with modifications (Li, Liu, Wang, Wang, Yang, & Wang, 2017). The temperature of oven was 30 °C. The mobile phase consisted of *n*-hexane, isopropanol and formic acid (21:1:0.003, v/v/v), and the flow rate was 1 mL/min. About 30 mg sample was dissolved in 1 mL of mobile phase and filtered through an organic membrane 0.22 μm for HPLC analysis. The chromatographic peaks were identified based on their retention times relative to known standards. The area normalization method was used to calculate the acylglycerol content according to the method of Li et al. (2016).

Slip melting point (SMP)

SMP was determined using capillary tubes according to the AOCS Official Method Cc 3–25 (AOCS, 2004). The sample was melted at 80 °C for 30 min, and the oil sample was aspirated with a capillary tube and incubated at –20 °C for 2 h. The capillary and thermometer were then connected and placed them in a beaker filled with ice water at 70 °C. Then, the thermometer reading was taken when test sample began to melt in the capillary tube.

Solid fat content (SFC) analysis

SFC of the sample was measured using Bruker Minispec pulsed nuclear magnetic resonance (pNMR) (MQ-20, Bruker, Karlsruhe, Germany). About 3 g of oil sample in an NMR tube was first melted at 80 °C for 30 min to eliminate crystal memory. Then it was incubated at 0 °C for 90 min. Finally, SFC was recorded at 5, 10, 15, 20, 25, 30, 35, 40 and 45 °C for 30 min at each temperature.

Rheological properties analysis

The rheological properties of sample were determined by an AR1500EX rheometer (AR1500EX, TA, USA) equipped with a parallel plate geometry (gap = 1 mm, diameter = 50 mm). The steady-shear rheological property was measured at a shear rate of 0–100 s⁻¹ within 2 min. The dynamic frequency sweep was conducted with a range of 0.01–100 Hz at 0.5% strain. The data of *G'* (storage modulus) and *G''* (loss modulus) were record, and the temperature was at 25 °C.

Thermodynamic properties analysis

Thermograms of melting and crystallization were determined using a differential scanning calorimetry (DSC) (DSC 214 Polyma, Netzsch, Germany) with nitrogen (99.99%) as the purge and protective gas at a flow rate of 50 mL/min. About 10 mg of oil sample was weighed and sealed into an aluminum pan. The cooling and melting conditions were as follows: increasing the temperature to 50 °C for 10 min to ensure complete melting of the sample, then decreasing to –30 °C at a rate of 5 °C/min and keeping for 10 min, finally, increasing to 70 °C at a rate of 5 °C/min. Meanwhile, melting and crystallization curves were recorded.

Crystal polymorphism analysis

Polymorphism was measured using an X-ray diffractometer (XRD, X'pert Power, Panalytical, Almelo, Netherlands). 30 mg of oil sample was heated to 80 °C for 30 min to remove pre-existing crystals, then it was cooled in a refrigerator at –18 °C for 2 h to form complete crystallization, finally was kept at 25 °C for 12 h. The analysis was conducted at a scan rate of 2 °/min with a 2θ range of 5–30° at room temperature (25 °C).

Preparation of Non-dairy creamer

Firstly, the emulsion was prepared with total solids of 30% (including wall and core materials) and 70% distilled water. Total solids

contained isomalto-oligosaccharides (IMO) (60%) and sodium caseinate (SC) (4%) as wall materials, and 34% DAG (50% CO-DAG) with 2% emulsifier (fatty acid esters/monostearate glycerides at 4:1, w/w) as core materials. Then the mixture was homogenized to obtain pre-emulsions by a shear homogenizer for 10 min at 10000 rpm. Then pre-emulsion was further homogenized for three times at 30 MPa in a high-pressure homogenizer (ATS-AH-MF1, Shanghai, China). Finally, the drying process was carried out using a spray dryer (SD-08, Wuxi, China) at inlet air temperature of 170 ± 2 °C.

Physicochemical characteristics of non-dairy creamer analysis

Microencapsulation efficiency. The microencapsulation efficiency of non-dairy creamer was evaluated according to the method by [Shamaei et al. \(2017\)](#). The surface oil content was measured using the organic solvent extraction method. About 0.5 g non-dairy creamer was weighed and 20 mL petroleum ether was added with shaking for 3 min. Then, the suspension was filtered and solid residues were re-extracted three times with 20 mL petroleum ether. The petroleum ether was removed by rotary evaporation. Finally, the extracted surface oil was dried in an oven at 105 °C until it reached a constant weight. The surface oil content was calculated according to the following equation:

$$\text{Surface oil(\%)} = \frac{\text{Extracted oil weight (g)}}{\text{Initial sample weight(g)}} \times 100 \quad (1)$$

The encapsulation efficiency of non-dairy creamer was defined as the ratio of encapsulated lipid to total lipid. The total oil content of non-dairy creamer was measured using the organic solvent extraction method. The encapsulation efficiency (ME) was calculated by the following equation:

$$\text{ME(\%)} = \frac{\text{Total oil} - \text{Surface oil}}{\text{Total oil}} \times 100 \quad (2)$$

Moisture Content. The moisture content of non-dairy creamer was measured according to the oven-drying method (AOAC 1997). The sample was weighed in a crucible and dried to a constant weight in an oven at 105 °C. Then the water content was calculated according to the mass loss of powder.

Solubility. The non-dairy creamer (W) was added to a 50 mL beaker with 38 mL of distilled water (25–30 °C). Then it was dissolved and transferred to a 50 mL centrifuge tube, and centrifuged at 4000 r/min for 10 min. This process was repeated until the nondairy creamer was no longer dissolved. Finally, the precipitate was transferred to an evaporating dish and dried to constant weight at 105 °C ([Santhalakshmy, Don Bosco, Francis, & Sabeena, 2015](#)). The solubility of non-dairy creamer was calculated by the following equation:

$$\text{Solubility (g/100g)} = 1 - \frac{W2 - W1}{(1 - B) \times W} \times 100 \quad (3)$$

(W: Mass of sample; W1: Mass of evaporating dish; W2: Mass of precipitate and evaporating dish; B: Water content of sample).

Wettability. The wettability of the non-dairy creamer was determined according to a method described by [Vissotto et al. \(2010\)](#). About 2 g non-dairy creamer was added to a 250 mL beaker filled with 200 mL of water at 25 °C, and the time was recorded when the powder was added until it was completely immersed in the water.

Angle of repose. The fluidity of non-dairy creamer was evaluated by the angle of repose. The angle of repose was measured using a modified method reported by [Zhu et al. \(2021\)](#). The correlation between the angle of repose and flowability is as follows: <30° indicates very good flowability of the product; 30° to 45° is considered good flowability; 45° to 60° means that the flowability of the product is moderate; >60° means that the product has poor flowability.

Scanning electron microscopy (SEM) graphs of different non-dairy creamers

The morphology of non-dairy creamer was determined using a SEM (S-3700 N, Hitachi Limited, Japan). The samples were set on a copper plate and sputtered with a gold layer for imaging. The morphology of the sample was observed at 15 kV acceleration voltage with magnifications of 200, 1000, and 3000 times.

Thermogravimetric (TG) analysis curve of different non-dairy creamers

The thermal stability of non-dairy creamer was analyzed using a thermogravimetric.

analyzer TG209F1 (Netzsch, Selb, Germany). Approximately 8–9 mg of sample was weighed in an aluminum pan and measured from 40 to 500 °C at a rate of 10 °C/min.

Fourier transform infrared (FTIR) spectrum of CO-DAG non-dairy creamer

The chemical structure of non-dairy creamer was characterized by a VERTEX 70 FTIR spectrometer (Bruker, Optics, Germany). About 10 mg of sample was analyzed using the KBr method according to [Sarabandi et al. \(2019\)](#), and FTIR spectra were measured with a scanning range of 4000—400 cm^{-1} .

Particle size distribution of non-dairy creamer in black coffee

The particle size distribution of non-dairy creamer in black coffee was determined by a Zetasizer nano series (Malvern, Worcestershire, UK) according to the method of [Long et al. \(2015\)](#). The refractive index of the dispersed phase (water) was set at 1.33, and the continuous phase was 1.45, respectively. The sample was measured at 25 °C.

Color of non-dairy creamer in black coffee

The chromatic values of coffee creamer, including L* (lightness), a* (redness-greenness) and b* (yellowness-blueness) were measured by Ultrascan VIS (Hunter Lab, USA) according to the CIE LAB system. Whiteness indices (WI) were calculated by the following equation:

$$\text{WI} = 100 - \sqrt{a^{*2} + b^{*2} + (100 - L^*)^2} \quad (4)$$

Statistical analysis

Each experiment was carried out in triplicate. All data were expressed as means \pm standard deviations. Data were evaluated using SPSS statistical 26 software by a one-way analysis of variance (ANOVA), and *t*-test was used to determine the significance of the differences among data at $p < 0.05$.

Results and discussion

Physicochemical characteristics of CO-DAG

Acylglycerol and fatty acid composition of CO-DAG

Table 1 shows the acylglycerol and fatty acid composition of CO and CO-DAG. CO mainly contained 97.01% TAG and 2.83% DAG. The dominant fatty acids in CO were lauric acid, myristic acid, caprylic acid, palmitic acid, and capric acid, which accounted for 49.32%, 17.83%, 8.27%, 8.08%, and 6.71% of total fatty acids (FAs), respectively. Similar observations were reported by [Moigradean et al. \(2013\)](#). CO-DAG exhibited a similar fatty acid composition to CO, with the highest lauric acid content (46.48–48.75%). Interestingly, the contents of oleic acid (C18:1) and linoleic acid (C18:2) of CO-DAG were slightly increased

Table 1
Acylglycerol and fatty acid composition of CO and CO-DAG.

	CO	30% CO-DAG	50% CO-DAG	70% CO-DAG	90% CO-DAG
Acylglycerol composition (%)					
TAG	97.01 ± 0.21 ^a	68.89 ± 0.37 ^b	48.57 ± 0.27 ^c	29.44 ± 0.11 ^d	9.75 ± 0.11 ^e
1,3-DAG	1.99 ± 0.12 ^c	23.01 ± 0.18 ^d	38.13 ± 0.15 ^c	52.28 ± 0.34 ^b	66.88 ± 0.31 ^a
1,2-DAG	0.84 ± 0.04 ^e	8.04 ± 0.13 ^d	13.27 ± 0.15 ^c	18.21 ± 0.15 ^b	23.30 ± 0.16 ^a
MAG	0.16 ± 0.06 ^a	0.06 ± 0.03 ^{ab}	0.03 ± 0.01 ^b	0.07 ± 0.01 ^{ab}	0.07 ± 0.02 ^{ab}
Fatty acid composition (%)					
Caprylic acid (C8:0)	8.27 ± 0.11 ^a	8.03 ± 0.08 ^b	7.55 ± 0.09 ^c	7.49 ± 0.12 ^c	6.95 ± 0.15 ^d
Capric acid (C10:0)	6.71 ± 0.08 ^a	6.58 ± 0.09 ^a	6.45 ± 0.06 ^b	5.98 ± 0.05 ^c	4.91 ± 0.03 ^d
Lauric acid (C12:0)	49.32 ± 0.48 ^a	48.75 ± 0.53 ^b	48.57 ± 0.38 ^b	47.62 ± 0.43 ^c	46.48 ± 0.32 ^d
Myristic acid (C14:0)	17.83 ± 0.25 ^a	17.91 ± 0.31 ^a	17.97 ± 0.31 ^a	17.97 ± 0.18 ^a	18.11 ± 0.31 ^a
Palmitic acid (C16:0)	8.08 ± 0.16 ^c	8.27 ± 0.31 ^d	8.62 ± 0.22 ^c	9.05 ± 0.25 ^b	9.76 ± 0.19 ^a
Stearic acid (C18:0)	3.15 ± 0.07 ^{bc}	3.22 ± 0.07 ^b	3.07 ± 0.06 ^c	3.18 ± 0.06 ^b	3.65 ± 0.07 ^a
Oleic acid (C18:1)	5.05 ± 0.14 ^c	5.82 ± 0.26 ^d	5.97 ± 0.15 ^c	6.73 ± 0.23 ^b	7.23 ± 0.12 ^a
C18:1-Trans	nd	nd	nd	nd	nd
Linoleic acid (C18:2)	0.85 ± 0.05 ^d	1.15 ± 0.04 ^c	1.12 ± 0.01 ^c	1.84 ± 0.01 ^b	2.47 ± 0.03 ^a
C18:2-Trans	nd	nd	nd	nd	nd
Others	0.75 ± 0.05 ^a	0.27 ± 0.03 ^c	0.68 ± 0.04 ^a	0.14 ± 0.02 ^d	0.44 ± 0.02 ^b

Mean ± standard deviation of determinations for triplicate sample. Different letters in the same row indicate significant differences at $p < 0.05$. nd: not detected.

compared with CO. This observation was different from the findings from Long et al. (2015), who found that the unsaturated fatty acid content (C18:1 and eicosenoic acid (C20:1)) of DAG-based peanut oil was lower than peanut oil. Probably, different enzymatic processes for the production of DAG have an influence on fatty acid composition. Particularly, trans fatty acids could not be detected in CO and CO-DAG.

Hardness and rheological properties of CO-DAG

In general, partially hydrogenated coconut oil has a higher melting point and is widely used for the preparation of non-dairy creamer. However, coconut oil is rarely used as a core material to prepare non-dairy creamer due to its relatively low melting point (24–28 °C). Therefore, it is essential to study the physicochemical properties of CO-DAG as a core material.

Fig. 1(A) shows the hardness of CO and CO-DAG. It was found that the hardness of CO-DAG increased as the DAG content increased. The hardness of CO and 30% CO-DAG were 0 and 1.36 g, respectively, indicating a liquid state at 25 °C. The hardness of 70% CO-DAG and 90% CO-DAG reached 198.79 g and 487.25 g, respectively, showing the form of a solid state at 25 °C. This result is similar to that reported by Xu, Wei, Zhao, Lu, and Dong (2016) who found that the hardness of palm-based DAG oil was higher than palm oil due to the stronger hydrogen bonds formed between free hydroxyl group in DAG. As shown in Fig. 1(B), the viscosity of different contents CO-DAG decreased rapidly as the increase of shear rate (0–30 s⁻¹), indicating a typical pseudoplastic fluid. Moreover, the curve of viscosity of CO-DAG became significantly slower and eventually reached equilibrium as the shear rate increased (30–100 s⁻¹), indicating a Newtonian fluid. The viscosity increased gradually with an increased DAG content at the same low shear rate, which was consistent with the result of Ng et al. (2014). The higher the viscosity of CO-DAG, the higher mechanical strength, which corresponded to the results of

hardness.

The effects of DAG content on viscoelastic properties can also be described by storage modulus (G' , the elastic property of CO-DAG) and loss modulus (G'' , the viscosity property of CO-DAG). Sample showed liquid-like properties when $G'' > G'$, while sample exhibited solid-like behavior when $G'' < G'$ (Xi, Liu, McClements, & Zou, 2019). The texture of fat relates to G' and G'' , the mouthfeel is less smooth when it exhibits more solid characteristics. As shown in Fig. 1(C), CO and 30% CO-DAG exhibited higher G'' than G' , which was a typical liquid-like behavior. Interestingly, G' increased rapidly as the DAG content increased from 30% to 50%, implying the occurrence of liquid–solid transition. Obviously, 50%, 70% and 90% CO-DAG showed solid-like properties (Fig. 1(D)). This might be due to the tight crystalline network structure of DAG which enhanced the elastic and solid behaviors (Lei, Zhang, Wan, Tan, & Qiu, 2019).

SFC of CO-DAG

The SFC profiles of CO and CO-DAG are shown in Fig. 1(E). SFC relates to the plasticity and texture of product. Generally, SFC at 0–10 °C determines the ductility and stability of fat at a low temperature, SFC at 20–25 °C reflects the resistance of oil exudation and plasticity of fat at room temperature, and SFC at 33–38 °C correlates with the mouthfeel of plastic fat (Meng et al., 2010). As shown in Fig. 1(E), CO showed a steep melting curve from 10 °C to 25 °C. However, the SFC of CO-DAG differed from CO, and the melting range expanded as DAG content increased, which was consistent with the lard DAG (Miklos, Zhang, Lametsch, & Xu, 2013). The SFC of 50% CO-DAG and 70% CO-DAG were 30.05 and 40.85% at 25 °C, and they were completely melted at 32 °C and 35 °C, respectively, indicating that they could prevent oil exudation at room temperature and melted quickly at oral temperature (37 °C). However, the SFC was 20.69% of 90% CO-DAG at 35 °C. These results demonstrated that CO-DAG with a high concentration of DAG contributed to an expanded plastic range of CO-DAG, however, excessive DAG will lead to high SFC to affect mouthfeel. Therefore, 50% and 70% CO-DAG have the potentials as alternative plastic fats.

Thermodynamic properties of CO-DAG

The melting crystallization curves of CO-DAG were analyzed using DSC to further investigate its thermodynamic properties. As shown in Fig. 1(F), CO exhibited one wide endothermic peak at 23.55 °C due to the different fatty acid compositions of TAG. Interestingly, CO-DAG exhibited two endothermic peaks according to the composition of acylglycerol, the peak (P1) corresponding to TAG component and the peak (P2) corresponding to DAG component with a high melting point, which were consistent with the results reported by Latip et al. (2013). Furthermore, as the DAG content increased, the endothermic peak on left (P1) gradually disappeared, while the peak (P2) shifted towards a high temperature range with a sharper shape. These results correspond to the observation by Miklos et al. (2013), who found that the onset points and melting peaks of lard-based DAG shifted towards the higher temperatures region with the increased content of DAG.

Fig. 1(G) shows the crystallization curves of CO and CO-DAG. CO exhibited two wide exothermic peaks at -3.43 °C and 2.61 °C, which was consistent with the observation that CO also had two exothermic peaks at -4.43 °C and 1.02 °C due to three saturated TAGs, i.e. C12:0/C12:0/C12:0, C8:0/C8:0/C12:0, C8:0/C12:0/C12:0, and C12:0/C12:0/C14:0. (Ng et al., 2021). As the content of DAG increased, the exothermic peak gradually disappeared around at 0 °C, whereas it became apparent at above 20 °C and shifted to a higher temperature range. Interestingly, 70% and 90% CO-DAG showed a sharp exothermic peak at 27.08 °C and 30.58 °C, respectively, indicating faster nucleation and growth of lipid crystals during the crystallization process. These results showed that DAG could facilitate the crystallization of CO-DAG through forming new nucleation sites. Similar observations were reported in lard-based DAG, which promoted crystal nucleation and growth as the concentration of DAG increased from 50% to 100%

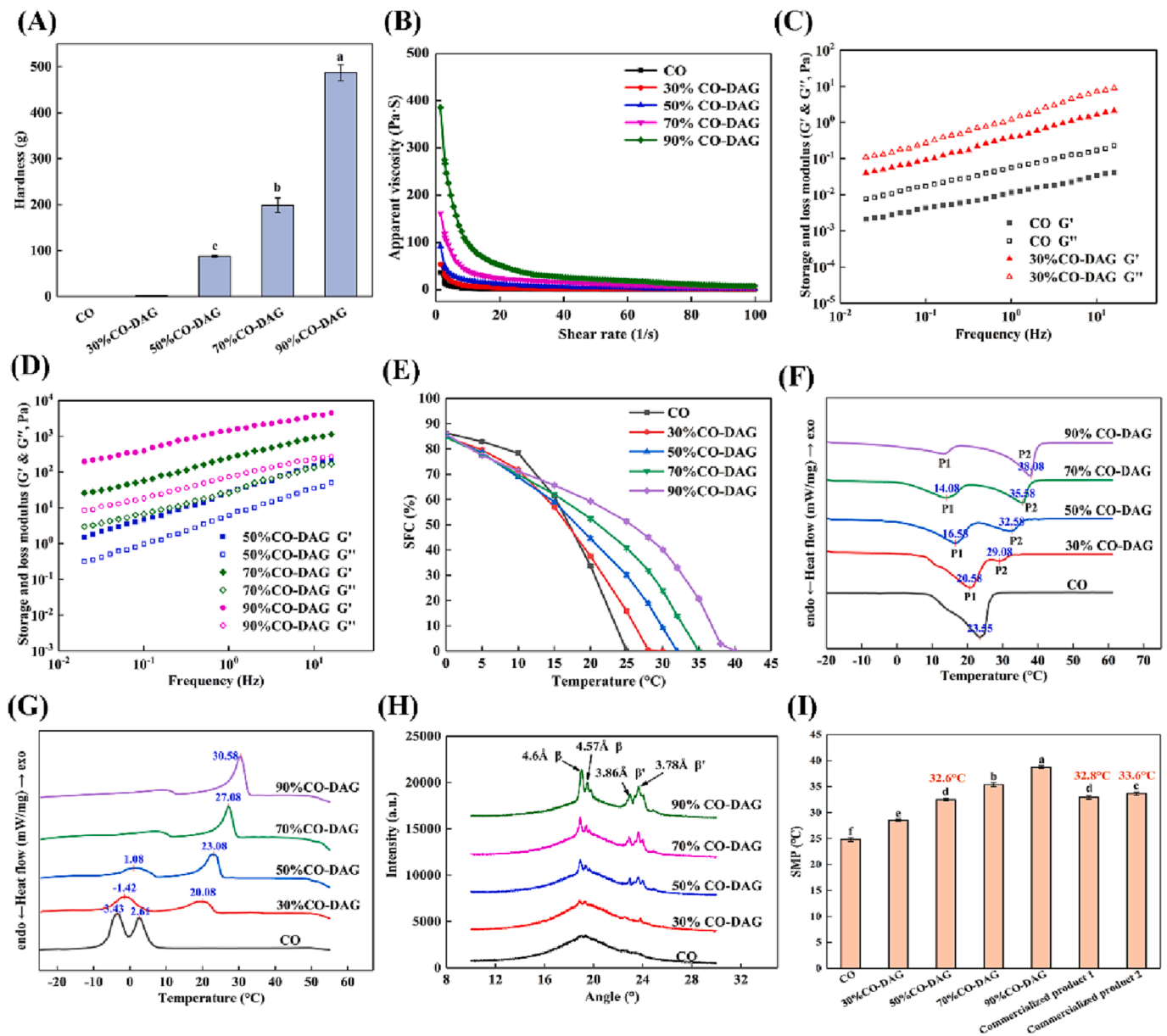


Fig. 1. Physicochemical characteristics of CO and CO-DAG. (A) Hardness of CO and CO-DAG; (B) Apparent viscosity of CO and CO-DAG; (C) Storage and loss modulus CO and CO-DAG; (D) Storage and loss modulus CO and CO-DAG; (E) SFC of CO and CO-DAG; (F) Melting properties of CO and CO-DAG; (G) Crystallization properties of CO and CO-DAG; (H) Crystal polymorphism of CO and CO-DAG; (I) SMP of CO and CO-DAG.

(Miklos, Zhang, Lametsch, & Xu, 2013).

Crystal polymorphism of CO-DAG

The polymorphic formation contributes to the sensory evaluation of product. The crystal behaviors of CO and CO-DAG (30, 50, 70 and 90%) are shown in Fig. 1(H). The short spacing observed at 4.56 Å and 4.60 Å represented the β form, while the β' form exhibited two short spacings at 3.78 Å and 3.86 Å, which were consistent with the observation of crystal polymorphisms in DAG-enriched palm olein (Xu, Zhao, Wang, Peng, & Dong, 2016). The crystal forms of CO and 30% CO-DAG were mainly in β form. However, short spacings appeared at 4.56 Å, 4.60 Å, 3.78 Å and 3.86 Å in 50, 70 and 90% CO-DAG, respectively, indicating the presence of a mixture of β and β' polymorphic forms. Nakajima et al. (2004) reported that the crystal forms of DAG were associated with the structure of DAG. Specifically, 1,3-DAG with symmetrical structure displayed β crystal form, whereas 1–2 DAG formed β' crystal form. As the DAG content increased, the short spacing at 3.86 Å and 3.78 Å became

intensified, indicating an increased β' form crystal due to the appearance of 1,2-DAG. The texture of fat product would be more delicate with the tighter crystal network structure of β' crystal form. In addition, fat products enriched with crystals in β' form are more suitable for the preparation of plastic fat to delay the formation of β in spread, contributing to the overall texture and a smooth surface (Miklos, Zhang, Lametsch, & Xu, 2013).

SMP of CO-DAG

The SMP relates to acylglycerol structure, composition of fatty acid, and the strength of hydrogen bonds between hydroxyl groups. As shown in Fig. 1(I), the SMP of 30% CO-DAG, 50% CO-DAG, 70% CO-DAG, and 90% CO-DAG were 24.8, 28.4, 32.6, 35.2, and 38.8 °C, respectively, which were in accordance with the results of SFC. The SMP increased as the DAG content increased.

The physicochemical characteristics of core material play critical roles in the applications of non-dairy creamer. SFC of 50% CO-DAG and

70% CO-DAG were 30.05% and 40.85% at 25 °C, which were completely melted at 32 °C and 35 °C, implying their prevention effects from oil exudation at room temperature and quick melting at the oral temperature of human. However, the SFC at the level of 20.69% of 90% CO-DAG at 35 °C could lead to a poor mouthfeel. The crystal polymorphism results exhibited the presence of a mixture of β and β' polymorphic forms in 50, 70 and 90 %CO-DAG. Generally, hydrogenated fats tend to form stable β crystal and uniform β' crystal to provide high plasticity and smooth mouthfeel. A high content of DAG (90%) may lead to brittle and sandy mouthfeel. These results suggested the potentials of 50% and 70% CO-DAG as potential core material for the production of non-dairy creamer. Furthermore, SMP of core material is a key factor in non-dairy creamer, and the melting point of 32 ~ 38 °C is vital for the texture and stability of non-dairy creamers (Wanthong & Klinkesorn, 2020). In our study, the SMP of commercial core materials were 32.8 °C and 33.6 °C, respectively. Interestingly, the SMP of 50% CO-DAG (32.6 °C) was close to that of the commercial non-dairy creamer (32.8 °C and 33.6 °C). Therefore, taking into consideration the SFC profiles, crystal polymorphism and SMP of CO-DAG, 50% CO-DAG was used as the core material for the preparation of non-dairy creamer.

Physicochemical characteristics of non-dairy creamer

Basic physicochemical properties of non-dairy creamer

As shown in Table 2, the basic physicochemical properties of CO-DAG and commercial non-dairy creamers were evaluated and

Table 2
Basic physicochemical properties of non-dairy creamer.

	CO-DAG-based non-dairy creamer	Commercial non-dairy creamer 1	Commercial non-dairy creamer 2
Surface oil content (%)	2.26 ± 0.03 ^a	2.01 ± 0.09 ^b	2.09 ± 0.05 ^{ab}
Total oil content (%)	31.12 ± 0.14 ^c	34.77 ± 0.11 ^a	32.93 ± 0.16 ^b
Encapsulation efficiency (%)	92.74 ± 0.11 ^b	94.22 ± 0.23 ^a	93.65 ± 0.17 ^{ab}
Moisture content (%)	1.78 ± 0.07 ^c	3.75 ± 0.06 ^a	3.59 ± 0.08 ^b
Solubility (g/100 g)	94.21 ± 0.22 ^c	96.38 ± 0.35 ^a	94.47 ± 0.51 ^b
Wettability (s)	12.08 ± 1.46 ^c	34.04 ± 1.89 ^b	49.54 ± 2.16 ^a
Angle of repose (°)	42.47 ± 1.01 ^a	27.18 ± 0.95 ^b	29.56 ± 1.46 ^b
Acylglycerol composition (%)			
TAG	48.57 ± 0.27 ^b	95.06 ± 0.21 ^a	95.60 ± 0.30 ^a
1,3-DAG	38.13 ± 0.15 ^a	2.82 ± 0.14 ^b	2.53 ± 0.14 ^b
1,2-DAG	13.27 ± 0.15 ^a	1.10 ± 0.06 ^c	1.46 ± 0.06 ^b
MAG	0.03 ± 0.01 ^c	0.75 ± 0.07 ^a	0.41 ± 0.05 ^b
Fatty acid composition (%)			
Caprylic acid (C8:0)	7.55 ± 0.09 ^a	3.81 ± 0.08 ^c	4.73 ± 0.08 ^b
Capric acid (C10:0)	6.45 ± 0.06 ^a	3.28 ± 0.08 ^c	3.96 ± 0.09 ^b
Lauric acid (C12:0)	48.57 ± 0.38 ^a	41.65 ± 0.15 ^c	42.09 ± 0.24 ^b
Myristic acid (C14:0)	17.97 ± 0.31 ^a	13.33 ± 0.08 ^c	14.07 ± 0.10 ^b
Palmitic acid (C16:0)	8.62 ± 0.22 ^c	10.41 ± 0.10 ^b	10.93 ± 0.08 ^a
Stearic acid (C18:0)	3.07 ± 0.06 ^c	26.73 ± 0.11 ^a	22.06 ± 0.12 ^b
Oleic acid (C18:1)	5.97 ± 0.15 ^a	0.30 ± 0.02 ^c	0.95 ± 0.04 ^b
C18:1-Trans	–	–	0.22 ± 0.09 ^a
Linoleic acid (C18:2)	1.12 ± 0.01 ^a	0.30 ± 0.02 ^b	0.25 ± 0.01 ^c
C18:2-Trans	–	–	0.16 ± 0.09 ^a
Others	0.68 ± 0.04 ^a	0.19 ± 0.03 ^b	0.57 ± 0.07 ^a

Mean ± standard deviation of determinations for triplicate sample. Different letters in the same row indicate significant differences at $p < 0.05$. nd: not detected.

compared. The total oil content and the encapsulation efficiency of CO-DAG-based non-dairy creamers were comparable with commercial non-dairy creamers, and encapsulation efficiency of three non-dairy creamers was all above 90%. It is well known that water content has a significant effect on non-dairy creamer to ensure product stability during shelf life (Vu, He, McClements, & Decker, 2020). The water content of CO-DAG (1.78%)-based non-dairy creamer was significantly lower than commercial non-dairy (3.5–4.0%) ($p < 0.05$), which was sufficient to guarantee the stability of product. Interestingly, a significant difference in the wettability of three non-dairy creamers ($p < 0.05$) was observed. The wetting time of CO-DAG-based non-dairy creamer (12.08 s) was shorter than that of the two commercial non-dairy creamers (34.04 s, 49.54 s). It was inferred that the unique hydroxyl structure of CO-DAG formed hydrogen bonds with water, thereby decreasing the wetting time (Zhu, Li, Liu, Li, Qi, & Jiang, 2021). The angle of repose is an important indicator to evaluate the flowability of non-dairy creamers. In this study, the angle of repose of CO-DAG non-dairy creamer was 42.47, exhibiting good flowability.

The acylglycerol and fatty acid composition of different non-dairy creamers

The acylglycerol and fatty acid composition of CO-DAG-based non-dairy creamers and commercial non-dairy are shown in Table 2. The acylglycerol composition of CO-DAG-based non-dairy creamer consisted of DAG (51.40%) and TAG (48.57%). However, the two commercial non-dairy creamers investigated in the current study contained mainly TAG, accounting for 95.06% and 95.60%, respectively. With respect to fatty acid compositions, lauric acid was the most abundant fatty acid in CO-DAG-based non-dairy creamers, accounting for 48.57%, followed by myristic acid (17.97%), palmitic acid (8.62%), caprylic acid (7.55) and capric acid (6.45%). It contained 7.09% unsaturated fatty acids. It is noteworthy that no trans fatty acids were identified. The fatty acid composition of the two commercial non-dairy creamers contained mainly lauric acid (41.65%, 42.09%), stearic acid (26.73%, 22.06%), myristic acid (13.33%, 14.07%) and palmitic acid (10.41%, 10.93%). The content of unsaturated fatty acids of commercial non-dairy creamers was only about 1%. It was inferred that the commercial non-dairy creamers consisted of partially hydrogenated oil, including 0.38% trans fatty acids in non-dairy creamer 2. Therefore, the CO-DAG serves as an alternative fat for the production of healthy non-dairy creamer without trans fatty acids.

SEM graphs of different non-dairy creamers

As shown in Fig. 2, the surface morphologies of CO-DAG-based non-dairy creamer and commercial non-dairy creamers were characterized by SEM. The overall distribution of two commercial non-dairy creamers could be observed at the magnification of 20 times, while CO-DAG non-dairy creamer could be observed at the magnification of 200 times, indicating that the particle size of CO-DAG-based non-dairy creamer was smaller than that of the commercial non-dairy creamers. A significant difference in the microstructure between CO-DAG-based and commercial non-dairy creamers was observed. The CO-DAG non-dairy creamer had a nearly spherical and smooth surface, which confirmed that CO-DAG was successfully encapsulated by wall material. This result was consistent with the encapsulation results of medium- and long-chain TAGs, which also had a smooth spherical morphology (Korma, Wei, Ali, Abed, Zheng, Jin, & Wang, 2019). However, commercial products exhibited an irregular structure with wrinkles on the surface of the particles. This phenomenon can be explained by different drying methods of microcapsules (Tolun, Altintas, & Artik, 2016).

TG of different non-dairy creamers

The thermal stability of non-dairy creamers was assessed using TG. As shown in Fig. 3(A-C), the TG curves of CO-DAG and commercial non-dairy creamers could be divided into three stages. The first stage of mass loss occurred when the water and volatile components were dehydrated at 50–150 °C. The weight loss was approximately 1.66, 4.08, and 4.30%

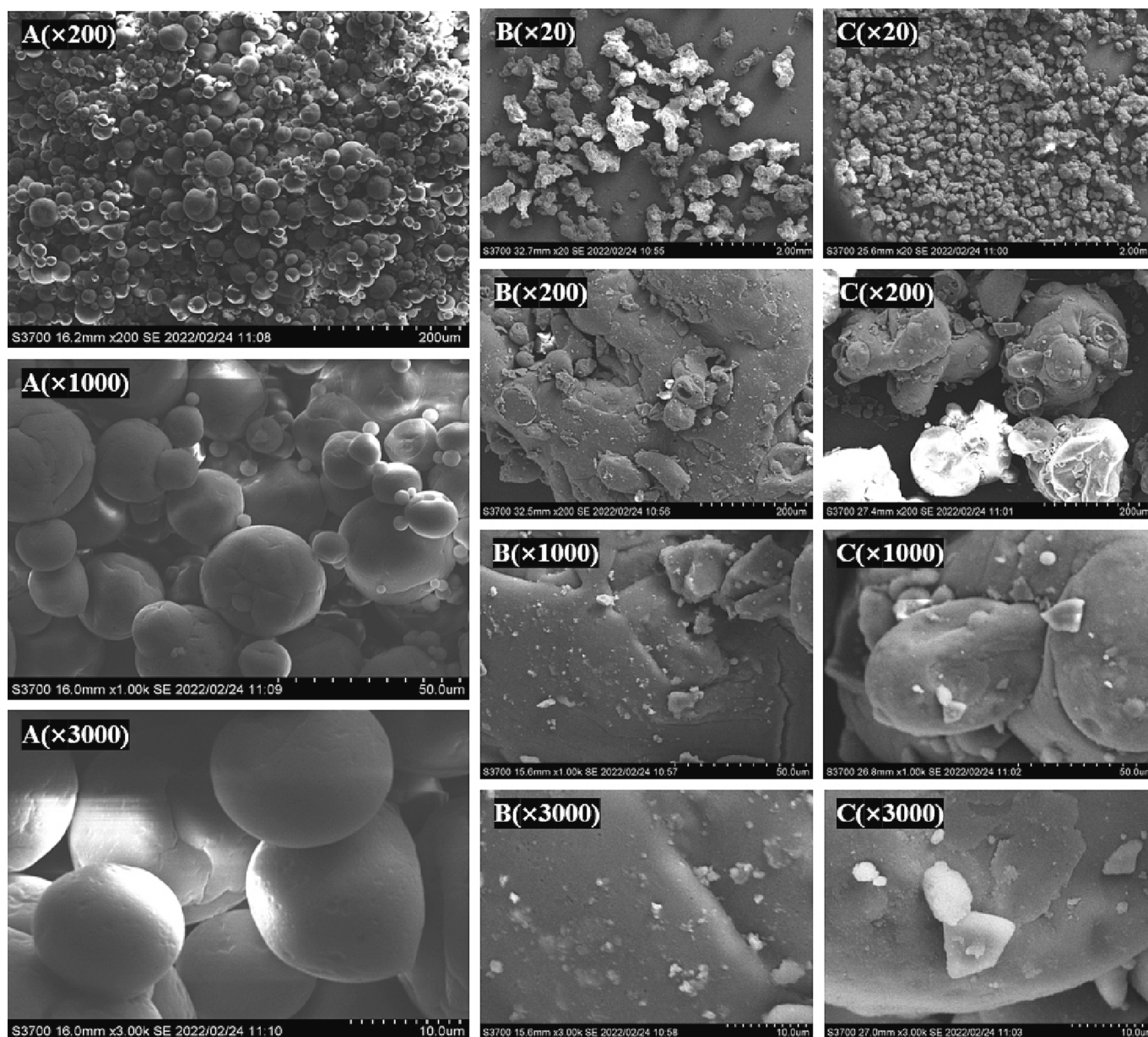


Fig. 2. SEM morphologies of different non-dairy creamers. A: CO-DAG non-dairy creamer; B: Commercial non-dairy creamer 1; C: Commercial non-dairy creamer 2.

of CO-DAG, commercial non-dairy creamer 1 and 2, respectively, which corresponded to the results of moisture content. In the second stage, a significant weight loss was observed between 150 and -280°C , with mass losses of 21.30, 19.46 and 15.83% for commercial non-dairy creamers 2, CO-DAG-based non-dairy creamer and commercial non-dairy creamer 1, respectively. This phenomenon could be explained by the decomposition of wall materials. In the third stage, the weight loss of three non-dairy creamers was approximately 50% when the temperature exceeded 280°C due to the decomposition of core and residual material. The TG curves demonstrated that CO-DAG-based non-dairy creamer exhibited similar thermal stability to commercial non-dairy creamers.

FTIR spectrum of CO-DAG non-dairy creamers

The FTIR spectra of CO-DAG, SC, IMO and CO-DAG non-dairy-based creamer are shown in Fig. 3(D). CO-DAG showed an absorption peak at 1735 cm^{-1} , representing the stretching vibration of $\text{C}=\text{O}$ of the ester carbonyl. The absorption peak at 2925 cm^{-1} and 2852 cm^{-1} were caused by the stretching of CH_3 and CH_2 , respectively. These characteristic peaks of CO-DAG-based were similar with the peak of CO-DAG

non-dairy creamer. From the spectra of wall material of SC and IMO, the absorption peak at about $3200\text{--}3500\text{ cm}^{-1}$ was associated with the stretching of $-\text{OH}$, and it was also observed in CO-DAG-based non-dairy creamer. The absorption peak at 1644 and 1515 cm^{-1} in SC represented the stretching vibration of $\text{C}=\text{O}$ and $\text{N}-\text{C}=\text{O}$, respectively. The absorbance at 1025 cm^{-1} in IMO was observed corresponding to the $\text{C}-\text{O}-\text{C}$ stretching. CO-DAG non-dairy creamer exhibited characteristic peaks of CO-DAG and wall material (SM and IMO), indicating that CO-DAG was successfully encapsulated by wall materials. Moreover, new chemical bonds were not found, which suggested that there was no significant interaction between CO-DAG and wall materials. These results are similar to those reported by Mohammed et al. (2019).

The application of CO-DAG-based non-dairy creamer in black coffee

Visual appearance

Non-dairy creamers are critical for black coffee whitening and desired creamy appearance. Fig. 4(A) shows the appearance of black coffee solutions using CO and commercial non-dairy creamers. The

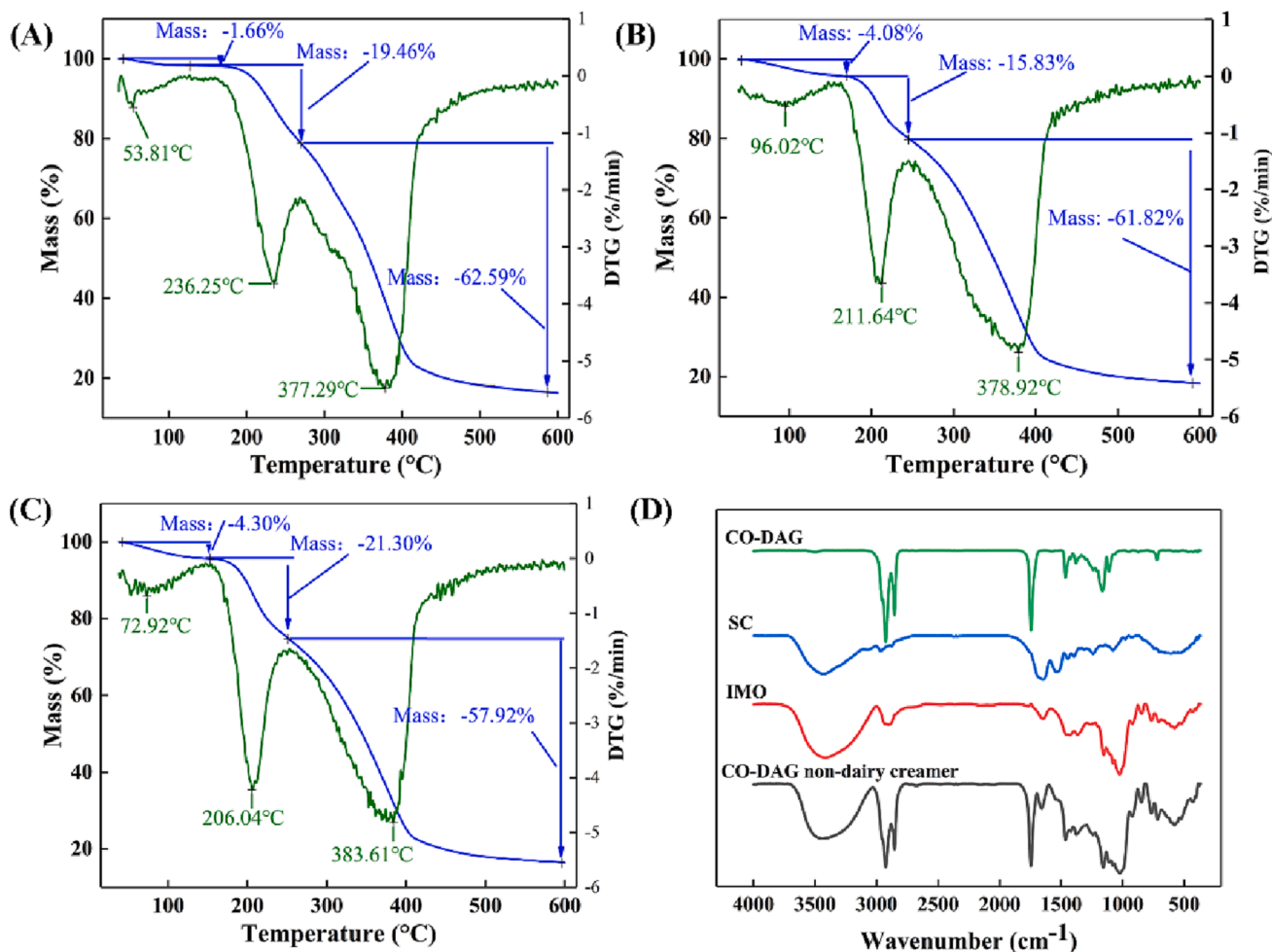


Fig. 3. Thermogravimetric and FTIR spectra analysis. (A) Thermogravimetric analysis of CO-DAG-based non-dairy creamer; (B) Thermogravimetric analysis of commercial non-dairy creamer 1; (C) Thermogravimetric analysis of commercial non-dairy creamer 1; (D) FTIR spectrum of CO-DAG-based non-dairy creamer and its component.

black coffee was brown in color, while the coffee solutions with CO-DAG-based non-dairy creamers were brownish-yellow which was similar to the coffee made of commercial non-dairy creamers. Therefore, CO-DAG-based non-dairy had a good whitening effect in blank coffee solution.

Particle size distribution

The application effect of CO-DAG-based non-dairy creamer in black coffee was evaluated. The particle size of the black coffee solution was 2.27 μm . Interestingly, the particle size of solution decreased rapidly to 0.63 μm when CO-DAG-based non-dairy creamer was added to black coffee. A similar observation was found in commercial non-dairy creamers ($d_{3,2}$, 0.67 and 0.69 μm). As shown in Fig. 4(B), the particle size distribution of blank coffee solution was more concentrated in the larger particle size region, and the coffee with commercial non-dairy creamers showed two peaks, indicating a non-uniform particle size distribution. However, the coffee with CO-DAG-based non-dairy creamer had only one peak and shifted towards the smaller particle size region, suggesting a stable and uniform distribution of CO-DAG-based non-dairy creamer in the black coffee solution. Similarly, the particle size of span in CO-DAG-based coffee creamer was smaller (3.47) than that of commercial non-dairy coffee creamer (4.96, 4.05). This suggested that CO-DAG had a more stable emulsion system due to the presence of hydrophilic hydroxyl groups in DAG. These results were consistent with Long et al. (2015), who found that peanut oil-based DAG emulsions showed higher stability due to the higher polarity of DAG.

Tristimulus color coordinate

To further investigate the effect of CO-DAG-based non-dairy creamer on the color of black coffee, and the values of L^* (lightness), a^* (redness-greenness) and b^* (yellowness-bluesness) of the coffee solution were determined by colorimeter (Fig. 4 (C-F)). As expected, there was a significant increase from 33.1 to 56.6 of the lightness in the black coffee solution as CO-DAG-based non-dairy creamer increased, which was similar to commercial non-dairy creamers. Interestingly, the redness (a^*) and yellowness (b^*) of coffee solution with addition creamers were higher than that of black coffee, which can be attributed to light scattering (Chung, Sher, Rousset, Decker, & McClements, 2017). a^* value of the coffee solution increased from 0.62 to 3.76, indicating a slight increase in the redness of the coffee solution with the addition of CO-DAG-based non-dairy creamer. Similarly, the yellowness (b^*) of black coffee became stronger with the addition of CO-DAG-based non-dairy creamer, with b^* value increasing from 1.69 to 16.20. However, further increased creamers resulted in decreased a^* and b^* values, which indicated decreased intensity in redness and yellowness. This result was consistent with Chung et al. (2017). The whiteness indices (WI) of coffee with CO-DAG and commercial non-dairy creamer 1 and 2 were 55.43, 54.2 and 50.22, respectively. The WI of the coffee with CO-DAG was similar to commercial non-dairy creamer 1, however, the WI of CO-DAG was higher than the commercial non-dairy creamer 2, indicating that CO-DAG had a good whitening effect for black coffee solutions.

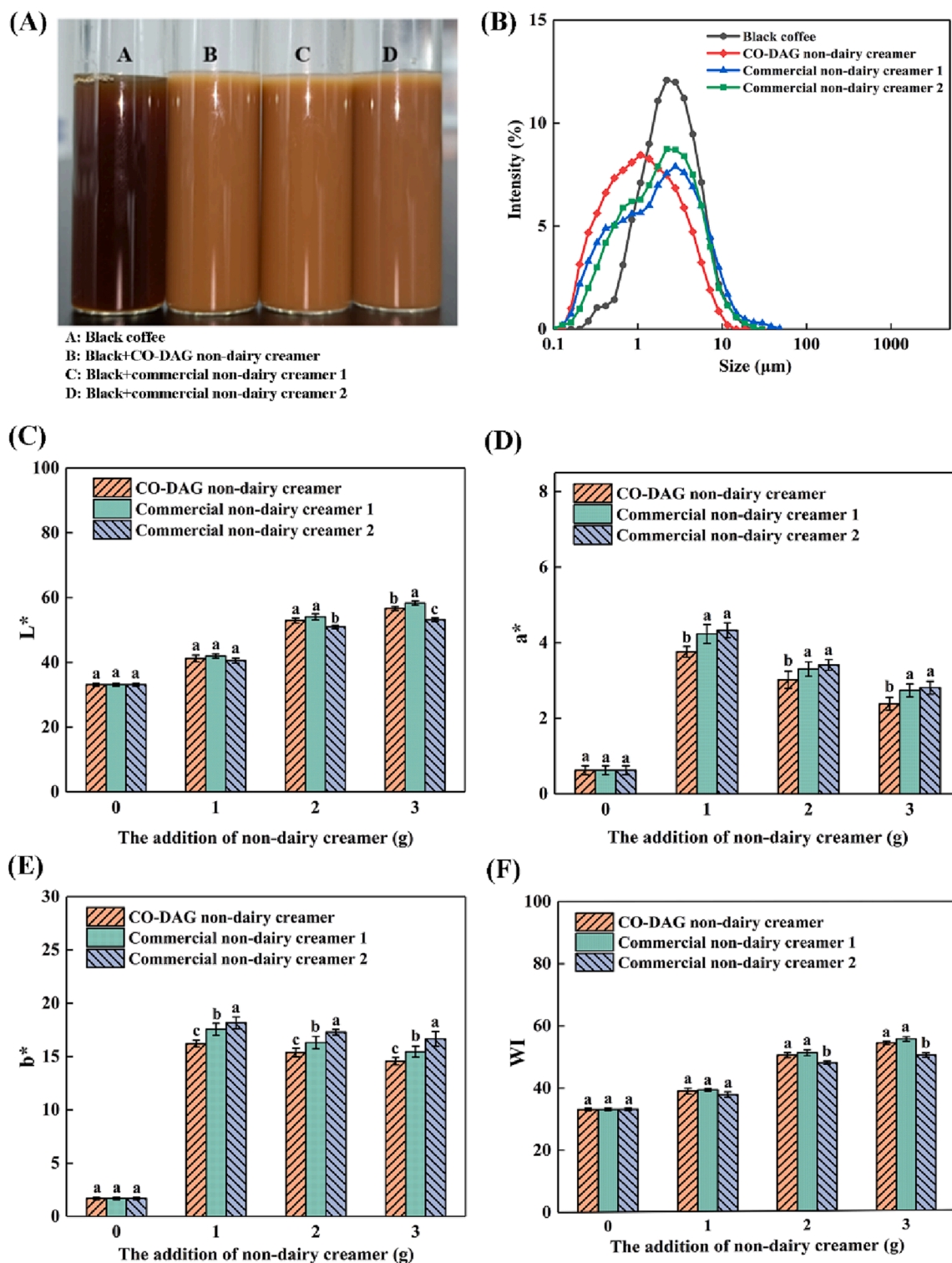


Fig. 4. The application of CO-DAG-based non-dairy creamer in black coffee. (A) Appearance of black coffee solutions with different non-dairy creamers; (B) Particle size distribution of different black coffee solutions; (C) L^* value; (D) a^* value; (E) b^* value; (F) Whiteness index.

Conclusions

In this study, an alternative fat blend CO-DAG with no trans fatty acids was used as core material to prepare non-dairy creamer and its performance in black coffee solutions was evaluated. As DAG content increased, the SFC, β' polymorphic forms and SMP of the CO-DAG increased due to the unique hydroxyl structure of CO-DAG. Taking into the SFC, crystal polymorphism and SMP of CO-DAG, 50% CO-DAG

was suitable core material for the preparation of non-dairy creamer. Besides, SEM analysis showed that CO-DAG non-dairy creamer had a nearly spherical and smooth surface, which demonstrated that CO-DAG was successfully encapsulated by wall material. CO-DAG-based non-dairy creamers exhibited similar encapsulation efficiency (92.74%) and good thermal stability to commercial products by TG analysis. Moreover, the CO-DAG based non-dairy creamer was applied to black coffee, and the whiteness index (54.20) was higher than commercial non-dairy

creamer 2 (50.22), suggesting that CO-DAG-based non-dairy creamer had a good whitening effect. Overall, 50% CO-DAG serves as a potential candidate of the core material for non-dairy cream containing no trans fatty acids, which is of great significance for the development of non-dairy creamer industry.

CRedit authorship contribution statement

Xuan Liu: Methodology, Formal analysis, Writing – original draft, Software. **Wanli Xu:** Methodology, Investigation, Formal analysis, Software. **Weifei Wang:** Conceptualization, Funding acquisition. **Riming Luo:** Funding acquisition. **Bo Yang:** Project administration. **Dongming Lan:** Funding acquisition. **Yonghua Wang:** Funding acquisition.

Declaration of Competing Interest

The authors declare that they have no known competing financial interests or personal relationships that could have appeared to influence the work reported in this paper.

Data availability

The authors do not have permission to share data.

Acknowledgements

This work was supported by the Guangdong Provincial Key R&D Programme (2022B0202010002); the Major science and technology projects in the Xinjiang Uygur Autonomous Region (2022A02004); China Agriculture Research System (CARS-18-ZJ0503) and Foshan Science and Technology Innovation (FS0AA-KJ919-4402-0013).

References

- Chung, C., Sher, A., Rousset, P., Decker, E. A., & McClements, D. J. (2017). Formulation of food emulsions using natural emulsifiers: Utilization of quillaja saponin and soy lecithin to fabricate liquid coffee whiteners. *Journal of Food Engineering*, 209, 1–11. <https://doi.org/10.1016/j.jfoodeng.2017.04.011>
- Dhaka, V., Gulia, N., Ahlawat, K. S., & Khatkar, B. S. (2011). Trans fats—sources, health risks and alternative approach-A review. *Journal of food science and technology*, 48(5), 534–541. <https://doi.org/10.1007/s13197-010-0225-8>
- Islam, M. A., Amin, M. N., Siddiqui, S. A., Hossain, M. P., Sultana, F., & Kabir, M. R. (2019). Trans fatty acids and lipid profile: A serious risk factor to cardiovascular disease, cancer and diabetes. *Diabetes & Metabolic Syndrome: Clinical Research & Reviews*, 13(2), 1643–1647. <https://doi.org/10.1016/j.dsx.2019.03.033>
- Korma, S. A., Wei, W., Ali, A. H., Abed, S. M., Zheng, L., Jin, Q., & Wang, X. (2019). Spray-dried novel structured lipids enriched with medium-and long-chain triacylglycerols encapsulated with different wall materials: Characterization and stability. *Food Research International*, 116, 538–547. <https://doi.org/10.1016/j.foodres.2018.08.071>
- Latip, R. A., Lee, Y. Y., Tang, T. K., Phuah, E. T., Tan, C. P., & Lai, O. M. (2013). Physicochemical properties and crystallisation behaviour of bakery shortening produced from stearin fraction of palm-based diacylglycerol blended with various vegetable oils. *Food Chemistry*, 141(4), 3938–3946. <https://doi.org/10.1016/j.foodchem.2013.05.114>
- Lee, W. J., Zhang, Z., Lai, O. M., Tan, C. P., & Wang, Y. (2020). Diacylglycerol in food industry: Synthesis methods, functionalities, health benefits, potential risks and drawbacks. *Trends in Food Science & Technology*, 97, 114–125. <https://doi.org/10.1016/j.tifs.2019.12.032>
- Lei, M., Zhang, N., Wan, J. L., Tan, C. P., & Qiu, C. (2019). Non-aqueous foams formed by whipping diacylglycerol stabilized oleogel. *Food Chemistry*, 312, Article 126047. <https://doi.org/10.1016/j.foodchem.2019.126047>
- Li, D., Liu, P., Wang, W., Wang, X., Yang, B., & Wang, Y. (2017). An Innovative Deacidification Approach for Producing Partial Glycerides-Free Rice Bran Oil. *Food and Bioprocess Technology*, 10(6), 1154–1161. <https://doi.org/10.1007/s11947-017-1896-1>
- Li, D., Wang, W., Qin, X., Li, X., Yang, B., & Wang, Y. (2016). A novel process for the synthesis of highly pure n-3 polyunsaturated fatty acid (PUFA)-enriched triglycerides by combined transesterification and ethanolysis. *Journal of Agricultural and Food Chemistry*, 64(34), 6533–6538. <https://doi.org/10.1021/acs.jafc.6b02675>
- Liu, X., Xu, L., Luo, R., Sun-Waterhouse, D., Liu, Z., Xu, Q., ... Wang, Y. (2022). Thermal properties, oxidative stability, and frying applicability of highly pure soybean-based diacylglycerol oil. *Journal of Food Processing and Preservation*, 46(5), e16528.
- Long, Z., Zhao, M., Liu, N., Liu, D., Sun-Waterhouse, D., & Zhao, Q. (2015). Physicochemical properties of peanut oil-based diacylglycerol and their derived oil-in-water emulsions stabilized by sodium caseinate. *Food Chemistry*, 184, 105–113. <https://doi.org/10.1016/j.foodchem.2015.03.052>
- Lu, H., Guo, T., Fan, Y., Deng, Z., Luo, T., & Li, H. (2020). Effects of diacylglycerol and triacylglycerol from peanut oil and coconut oil on lipid metabolism in mice. *Journal of Food Science*, 85(6), 1907–1914. <https://doi.org/10.1111/1750-3841.15159>
- Meng, Z., Liu, Y. F., Jin, Q. Z., Huang, J. H., Song, Z. H., Wang, F. Y., & Wang, X. G. (2010). Characterization of Graininess Formed in All Beef Tallow-Based Shortening. *Journal of Agricultural and Food Chemistry*, 58(21), 11463–11470. <https://doi.org/10.1021/jf102496p>
- Miklos, R., Zhang, H., Lametsch, R., & Xu, X. (2013). Physicochemical properties of lard-based diacylglycerol oils in blends with lard. *Food Chemistry*, 138(1), 608–614. <https://doi.org/10.1016/j.foodchem.2012.10.070>
- Mohammed, N. K., Tan, C. P., Manap, A., Yazid, M., Muhiaddin, B. J., & Meor Hussin, A. S. (2019). Production of functional non-dairy creamer using *Nigella sativa* oil via fluidized bed coating technology. *Food and Bioprocess Technology*, 12(8), 1352–1365. <https://doi.org/10.1007/s11947-019-02294-y>
- Moigradean, D., Poiana, M. A., Alda, L. M., & Gogoasa, I. (2013). Quantitative identification of fatty acids from walnut and coconut oils using GC-MS method. *Journal of Agroalimentary Processes and Technologies*, 19(4), 459–463.
- Nakajima, Y., Fukasawa, J., & Shimada, A. (2004). Physicochemical properties of diacylglycerol. *Diacylglycerol oil*, 182–196.
- Ng, S. P., Khor, Y. P., Lim, H. K., Lai, O. M., Wang, Y., Wang, Y., ... Tan, C. P. (2021). In-depth characterization of palm-based diacylglycerol-virgin coconut oil blends with enhanced techno-functional properties. *LWT - Food Science and Technology*, 145, Article 111327. <https://doi.org/10.1016/j.lwt.2021.111327>
- Ng, S. P., Lai, O. M., Abas, F., Lim, H. K., & Tan, C. P. (2014). Stability of a concentrated oil-in-water emulsion model prepared using palm olein-based diacylglycerol/virgin coconut oil blends: Effects of the rheological properties, droplet size distribution and microstructure. *Food Research International*, 64, 919–930. <https://doi.org/10.1016/j.foodres.2014.08.045>
- Ramesh, S. V., Krishnan, V., Praveen, S., & Hebbar, K. B. (2021). Dietary prospects of coconut oil for the prevention and treatment of Alzheimer's disease (AD): A review of recent evidences. *Trends in Food Science & Technology*, 112, 201–211. <https://doi.org/10.1016/j.tifs.2021.03.046>
- Santhalakshmy, S., Don Bosco, S. J., Francis, S., & Sabeena, M. (2015). Effect of inlet temperature on physicochemical properties of spray-dried jamun fruit juice powder. *Powder Technology*, 274, 37–43. <https://doi.org/10.1016/j.powtec.2015.01.016>
- Sarabandi, K., Jafari, S. M., Mahoonak, A. S., & Mohammadi, A. (2019). Application of gum Arabic and maltodextrin for encapsulation of eggplant peel extract as a natural antioxidant and color source. *International journal of biological macromolecules*, 140, 59–68. <https://doi.org/10.1016/j.ijbiomac.2019.08.133>
- Shamaei, S., Seiedlou, S. S., Aghbashlo, M., Tsotsas, E., & Kharaghani, A. (2017). Microencapsulation of walnut oil by spray drying: Effects of wall material and drying conditions on physicochemical properties of microcapsules. *Innovative Food Science & Emerging Technologies*, 39, 101–112. <https://doi.org/10.1016/j.ifset.2016.11.011>
- Soo, Y. N., Tan, C. P., Tan, P. Y., Khalid, N., & Tan, T. B. (2021). Fabrication of oil-in-water emulsions as shelf-stable liquid non-dairy creamers: Effects of homogenization pressure, oil type, and emulsifier concentration. *Journal of the Science of Food and Agriculture*, 101(6), 2455–2462. <https://doi.org/10.1002/jsfa.10871>
- Teng, M., Zhao, Y. J., Khoo, A. L., Yeo, T. C., Yong, Q. W., & Lim, B. P. (2020). Impact of coconut oil consumption on cardiovascular health: A systematic review and meta-analysis. *Nutrition reviews*, 78(3), 249–259. <https://doi.org/10.1093/nutrit/nuz074>
- Tolun, A., Altintas, Z., & Artik, N. (2016). Microencapsulation of grape polyphenols using maltodextrin and gum arabic as two alternative coating materials: Development and characterization. *Journal of Biotechnology*, 239, 23–33. <https://doi.org/10.1016/j.jbiotec.2016.10.001>
- Vissotto, F., Jorge, L., Makita, G., Rodrigues, M., & Menegalli, F. (2010). Influence of the process parameters and sugar granulometry on cocoa beverage powder steam agglomeration. *Journal of Food Engineering*, 97(3), 283–291. <https://doi.org/10.1016/j.jfoodeng.2009.10.013>
- Vu, T. P., He, L., McClements, D. J., & Decker, E. A. (2020). Effects of water activity, sugars, and proteins on lipid oxidative stability of low moisture model crackers. *Food Research International*, 130, Article 108844. <https://doi.org/10.1016/j.foodres.2019.108844>
- Wang, B., & Liu, J. (2014). Trans-free nondairy creamer prepared from enzymatic interesterification of soybean oil and fully hydrogenated soybean oil. *Journal of Food Process Engineering*, 37(4), 339–348. <https://doi.org/10.1111/jfpe.12090>
- Wang, X., Qin, X., Li, D., Yang, B., & Wang, Y. (2017). One-step synthesis of high-yield biodiesel from waste cooking oils by a novel and highly methanol-tolerant immobilized lipase. *Bioresource Technology*, 235, 18–24. <https://doi.org/10.1016/j.biortech.2017.03.086>
- Wanthon, T., & Klinkesorn, U. (2020). Rambutan (*Nephelium lappaceum*) kernel olein as a non-hydrogenated fat component for developing model non-dairy liquid creamer: Effect of emulsifier concentration, sterilization, and pH. *Journal of Food Science and Technology*, 57(12), 4404–4413. <https://doi.org/10.1007/s13197-020-04477-4>
- Xi, Z., Liu, W., McClements, D. J., & Zou, L. (2019). Rheological, structural, and microstructural properties of ethanol induced cold-set whey protein emulsion gels: Effect of oil content. *Food Chemistry*, 291, 22–29. <https://doi.org/10.1016/j.foodchem.2019.04.011>
- Xu, Y., Wei, C., Zhao, X., Lu, C., & Dong, C. (2016). A comparative study on microstructure, texture, rheology, and crystallization kinetics of palm-based diacylglycerol oils and corresponding palm-based oils. *European Journal of Lipid*

- Science and Technology*, 118(8), 1179–1192. <https://doi.org/10.1002/ejlt.201500369>
- Xu, Q., Qin, X., Lan, D., Liu, X., Yang, B., Liao, S., ... Wang, Y. (2022). Water-in-oil emulsions enriched with alpha-linolenic acid in diacylglycerol form: Stability, formation mechanism and in vitro digestion analysis. *Food Chemistry*, 391, Article 133201. <https://doi.org/10.1016/j.foodchem.2022.133201>
- Xu, Y., Zhao, X., Wang, Q., Peng, Z., & Dong, C. (2016). Thermal profiles, crystallization behaviors and microstructure of diacylglycerol-enriched palm oil blends with diacylglycerol-enriched palm olein. *Food Chemistry*, 202, 364–372. <https://doi.org/10.1016/j.foodchem.2016.01.102>
- Zhu, J., Li, X., Liu, L., Li, Y., Qi, B., & Jiang, L. (2021). Preparation of spray-dried soybean oil body microcapsules using maltodextrin: Effects of dextrose equivalence. *LWT - Food Science and Technology*, 154, Article 112874. <https://doi.org/10.1016/j.lwt.2021.112874>